LIMNOLOGY and OCEANOGRAPHY: METHODS

ASLO

Limnol. Oceanogr.: Methods 19, 2021, 293–302

doi: 10.1002/lom3.10423

In-air one-point calibration of oxygen optodes in underway systems

Meike Becker [1,2]* **Are Olsen** [1,2] **Gilles Reverdin** [3]

[1]Geophysical Institute, University of Bergen, Bergen, Norway
[2]Bjerknes Center for Climate Research, Bergen, Norway
[3]LOCEAN - Laboratoire d'Océanographie et du Climat: Expérimentations et Approches Numériques, Paris, France

Abstract

Ships of opportunity are a frequently used platform in surface ocean carbon observations and estimating the annual ocean carbon sink. For understanding the drivers behind changes in the ocean carbon system, oxygen measurements alongside the carbon dioxide measurements can be a valuable tool. We developed an in-air calibration system for oxygen optodes in underway systems. The regular measurements of atmospheric oxygen enable us to correct for sensor drift and biofouling. This new system can help to obtain reliable oxygen data from underway applications, especially if the vessel is not easily accessible and a frequent recalibration of the optode is not feasible.

Measuring the ocean carbon and oxygen distribution is a good way to estimate the biogeochemical state of the world's oceans and their response to a changing climate. For this, bottle measurements aboard research vessels cannot provide sufficient temporal and spatial coverage as they are neither time nor cost efficient enough. In response, technical solutions and platforms for autonomous measurements have been developed for both of these variables.

The solution for high precision measurements of carbon dioxide (CO_2) is a rather large system based on the absorption in the infrared part of the radiation spectrum by a sample of headspace gas that has been brought into equilibration with a large volume of seawater (Takahashi 1961), returning readings of the partial pressure of CO_2 (pCO_2) in water. These systems are usually installed on research vessels or commercial ships, so called Ships of opportunity (SOOP) (Pierrot et al. 2009; Bakker et al. 2016), but some types are also installed on larger surface moorings and sail drones (Friederich et al. 1995). Recently, pH sensors have been deployed on Argo floats (Johnson et al. 2016), enabling calculation of pCO_2 when combined with estimates of total alkalinity (Williams et al. 2017). However, these sensors do not yet reach the same accuracy as the shipboard systems.

Autonomous measurements of dissolved oxygen in the ocean are usually conducted using oxygen optodes, which are based on luminescence quenching (Tengberg et al. 2003). The optodes are much smaller than the pCO_2 systems, have less power consumption, do not use external standards, and are therefore widely used for profiling applications on floats or on gliders (Körtzinger et al. 2005; Bushinsky et al. 2016; Johnson et al. 2017). These oxygen measurements are an important component of the biogeochemical Argo program (Gruber et al. 2010; Roemmich et al. 2019). As such, most standard operating procedures developed for oxygen optodes focus on installations on floats and moorings (Bittig et al. 2015, 2018*a*). For the installation of floats, where the optodes are in the field for a long time without the possibility to recalibrate them, in-air calibration procedures were developed in order to track the sensor drift at 100% oxygen saturation (Bushinsky and Emerson 2013; Johnson et al. 2015; Bittig and Körtzinger 2017). These procedures are now implemented on a routine basis.

Optodes are also installed alongside the pCO_2 instruments on many SOOP lines. Although the accessibility is better than on a float, this application is associated with a set of challenges that can limit the accuracy of the measurements. The sensors experience large temperature variations (5–50°C), and are exposed to intense vibrations, as they are typically installed in the engine room of these various vessels. Water for analysis is drawn from a surface intake, making the installation prone to biofouling, which can cause nonlinear drift. While the predeployment drift rate can be as high as several percent per year (D'Asaro and McNeil 2013), the sensor drift in many factory calibrated optodes in float applications was found to be about 0.6% yr^{-1} (Bittig et al. 2018*a*). With this drift, recalibrating the sensor on an annular basis will not be enough to reach a target precision as within the Argo program of 0.5% (Gruber et al. 2010), especially if a potentially nonlinear drift caused by biofouling is added upon the sensor drift. Another factor

*Correspondence: meike.becker@uib.no

that might lead to an increased instrument drift of the optode in a SOOP installation compared to a float is the increased number of measurements. On a SOOP, the optodes are often measuring continuously which will lead to a faster degradation of the foil. While the sensor can be exchanged more frequently, this is often impractical, and recalibration can be costly. In situ reference sampling is complicated and cannot be expected from the ship's crew; let alone by a scientist onboard given the hazardous chemicals involved combined with very basic and makeshift, if any, facilities for laboratory work onboard these commercial vessels. Routines and equipment for regular validation of the sensor's performance during deployment are needed in order to provide high quality measurements at any point in time.

We developed an in-air calibration system for the application in underway systems. In this article, we will give an overview about the technical setup, our adjustments to the data reduction routines suggested by (Bittig et al. 2018*a*), and the performance of the optode during the first deployment.

Materials and procedures

We installed our in-air calibration system on the container vessel M/V Nuka Arctica (Royal Arctic Lines/Greenland). The vessel has had a pCO_2 system installed since 2004 and is regularly sailing from Aalborg, Denmark to Ilulissaat, Greenland, crossing the northern North Sea, the subpolar North Atlantic, and calling several ports along the west coast of Greenland. This means that it covers several water masses and large gradients in temperature, salinity, and biogeochemical properties during each transect. In this work, we show data from five transects during the first deployment of the oxygen calibration system in September/October 2018. An overview of the sailing region of Nuka Arctica and the sea surface temperature (SST) and Sea Surface Salinity (SSS) measured during those transects is given in Fig. 1.

Instrumentation

The measurement system on Nuka Arctica is installed underneath the water line in the engine room. It consists of a factory multipoint calibrated oxygen optode (4330, Aanderaa, Xylem, U.S.A.), a pCO_2 system (General Oceanics, U.S.A.) (measuring sea surface pCO_2 and atmospheric xCO_2), an intake temperature sensor (model 1524, Fluke, The Netherlands), and a thermosalinograph (SBE 21, Sea-Bird, U.S.A.). The air pressure inside the engine room is measured by a separate pressure sensor (DPS-81HB-TA, GE Measurement & Control Solutions, U.S.A.). The water flow over the intake temperature sensor and the thermosalinograph is 50–60 L min^{-1}. The water supply to the pCO_2 system and the optode is teed off this main line, at a rate of 2–3 L min^{-1}. After analysis, waters from these two instruments are drained into a tank by gravity. This drain tank is emptied overboard when full, approximately every 15 min. The optode is installed in the oxygen optode assembly kit from General Oceanics, which is a cylindrical PVC housing with an approximate volume of 1 L. The optode is operating with a sampling interval of 30 s. The general setup of the system installed on Nuka Arctica is described in more detail in Olsen et al. (2008) and Fröb et al. (2019).

For enabling in-air measurements, we connected the atmospheric overflow from the pCO_2 system to the drain of the optode housing. The intake for atmospheric air is located at the bow of the vessel, about 10 m over the sea surface. The pCO_2 system is pumping in atmospheric air continuously to keep the atmospheric line flushed but is only measuring atmospheric air for a few minutes every 3 h. The air is thus normally exiting via a ballast chamber. A schematic setup of the installation and a picture of the in-air calibration system for the optode is shown in Fig. 2. In seawater mode, the three-way valve (1) lets water into the optode housing. The air intake to the optode (2) is closed and the air vent valve (3) is open. Once a day the three-way valve 1 switches from water supply to air drain and valves 2/3 switch to direct the atmospheric air into the optode housing. This drains the water out of the optode housing and flushes it with atmospheric air when the 20 min of air measurements are conducted. The positions of the valves are continuously reported to the computer of the pCO_2 system and recorded there. The optode, for which results are reported here, was factory calibrated before (May 2018) and after (March 2019) deployment, which enables comparison of the drift determined using the two approaches. The salinity data were quality controlled and calibrated according to Alory et al. (2015) and can be accessed via the LEGOS website (http://www.legos.obs-mip.fr/observations/sss/datadelivery/dmdata).

Calculations

The drift of the optode with time can be described by the following equation, where the slope m is the time-dependent drift of the optode at 100% saturation.

$$pO_2 = m \times pO_{2;\mathrm{obs}} \tag{1}$$

Although we are using a multipoint calibrated optode, there is likely a remaining temperature dependence of the sensor. This can be quantified and correct for by introducing a $pO_2 - T$-slope a (Bittig et al. 2018*a*),

$$pO_2 = m \times \left(pO_{2;\mathrm{obs}} + a \times \left(T_{\mathrm{optode}} - 10^{\circ}\mathrm{C}\right)\right) \tag{2}$$

where T_{optode} is the temperature measured by the optode. For the in-air measurements, pO_2 equals the partial pressure of oxygen in atmospheric air, $pO_{2;\,\mathrm{air}}$, ($pO_2 = pO_{2;\,\mathrm{air}}$). Equation 2 can then be resolved into:

$$pO_{2;\mathrm{obs}} = \frac{1}{m} \times pO_{2;\mathrm{air}} - a \times \left(T_{\mathrm{optode}} - 10^{\circ}\mathrm{C}\right) \tag{3}$$

The challenge with this approach is to precisely determine the $pO_{2;\,\mathrm{air}}$ at the optode foil. The $pO_{2;\,\mathrm{air}}$ is dependent on the

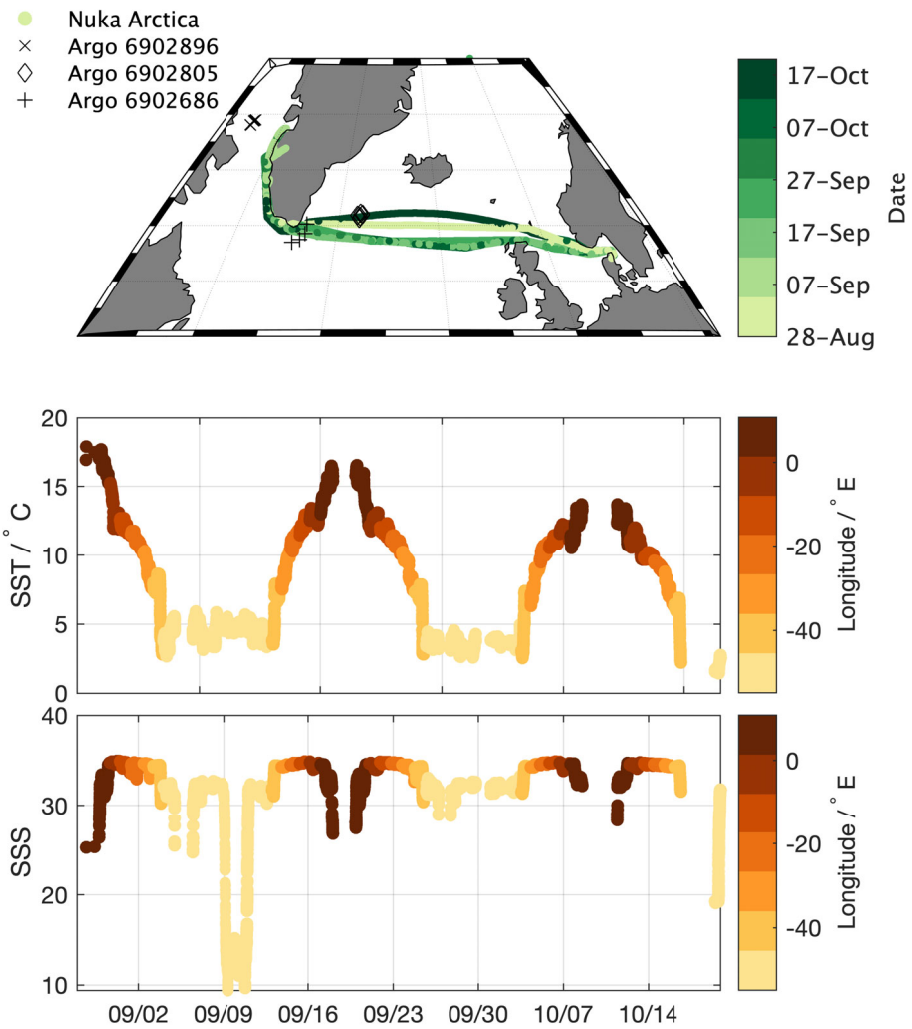

Fig. 1. Map showing the track of M/V Nuka Arctica and the surface temperature and salinity collected at five crossings during September/October 2018. Eastern parts are associated with warm and saline waters, while waters are colder and fresher in the west. The positions of the three Argo floats that were used for comparison are shown in black in the map.

mole fraction of oxygen in dry atmospheric air, xO_2, (xO_2 = 0.20946; Glueckauf 1951), the atmospheric pressure p_{atm}, and the partial pressure of water at the optode foil pH_2O_{foil}.

$$pO_{2;air} = xO_2 \left(p_{atm} - pH_2O_{foil}\right) \quad (4)$$

On floats, optodes can be submerged into seawater during the in-air measurements and measure a mixture of atmosphere and seawater. This is taken into account by introducing a factor for the so-called carry-over effect into the calculations. In our setup, the optode housing is completely emptied once valve 1 is open to the drain. Therefore, we do not have to consider the carry over effect. To be sure that we only took actual air measurements into the analysis, we dismissed the first measurement of each calibration period if it was differing more than 0.5% from the rest of the period. This also reduces the effect of rapid warming of the optode due to the difference between seawater temperature and room temperature. The temperature in the seawater varies between 2°C and 17°C, while the room temperature varies between about 5°C and 30°C. Once the optode housing is emptied for water, the optode starts warming. This can introduce a temperature gradient between the foil and the optode temperature sensor. By removing the very first datapoints, we minimize the influence of this on the final calibration.

One major source of uncertainty is the determination of pH_2O at the optode foil. Optimally, one would want to measure the humidity and temperature in the optode housing or directly after. Installing a water vapor sensor in the optode housing is not feasible as the housing is filled with seawater during most of the time. Therefore, we have to estimate the actual pH_2O inside the optode housing. Since this pH_2O_{foil} is a combination of the pH_2O of the air that is pumped into the chamber, pH_2O_{atm}, and additional water that is evaporating

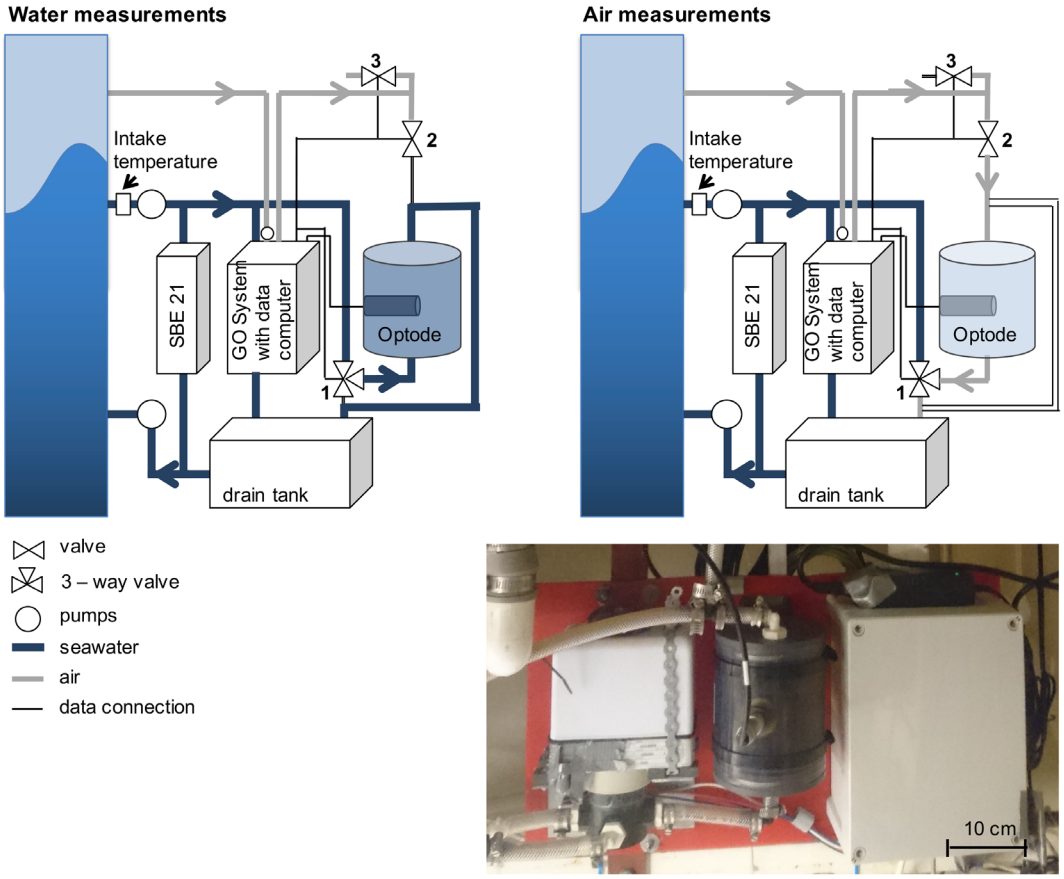

Fig. 2. Schematic setup of the optode in-air calibration system on Nuka Arctica during water measurements (left-hand side), during air measurements (right-hand side), and a picture of the installation.

from the wet walls of the chamber, installing a humidity sensor in the gas line before it enters the optode housing will not give the required $pH_2O_{foil.}$ either. We have considered a few different ways of estimating the pH_2O_{foil}: (1) assuming that the evaporation in the optode housing is so strong that we can use 100% humidity at the optode temperature for calculating $pH_2O_{sat,opt}$ (Eq. 5); (2) neglecting the evaporation in the optode housing and calculating the $pH_2O_{sat,SST}$ from 100% humidity at SST (Eq. 6); and (3) neglecting the evaporation inside the chamber and calculating the $pH_2O_{sat,NCEP/DOE\ II,}$ by using relative humidity (HUM) and air temperature data from the NCEP/DOE AMIP-II reanalysis (Eq. 6).

$$pO_{2;air} = xO_2\left(p_{atm} - pH_2O_{sat,opt}\right) \quad (5)$$

$$pO_{2;air} = xO_2\left(p_{atm} - pH_2O_{sat,SST}\right) \quad (6)$$

$$pO_{2;air} = xO_2\left(p_{atm} - pH_2O_{sat,NCEP/DOE\ II} \times HUM\right) \quad (7)$$

Method 1 assumes that the air pumped through the optode housing reaches 100% humidity while being pumped through optode housing. Method 2 has the uncertainty of neglecting evaporation in the optode housing and assuming 100% humidity outside the vessel. Method 3 also neglects the evaporation in the optode housing. In addition, method 3 introduces an error through combining in situ measurements with a gridded reanalysis product (2.5°×2.5°).

$pO_{2;\ obs}$ can be calculated from the oxygen concentration (c_{O_2}), reported by the factory calibrated optode, according to (Bittig et al. 2018*a*). For surface measurements (hydrostatic pressure of 0), we get:

$$pO_{2;obs} = c_{O_2}\left(T_{optode}, S_{preset}\right) \times \frac{xO_2(1013.25 - pH_2O_{sat})}{T_{Corr,optode}} \quad (8)$$

where T_{optode} is the temperature recorded by the optode; S_{preset}, the salinity used in the internal calculation in the optode (in our case 0); $T_{Corr,optode}$, the temperature correction based on the optode temperature; and $pH_2O_{sat,}$ the partial pressure of H_2O at 100% humidity (T_{optode}, S_{preset}).

Now that we have determined $pO_{2;\ obs}$ and $pO_{2;\ air}$ for each in-air measurement, we can use these together with the optode temperature T_{optode} and solve Eq. 3 for its two unknowns, m and a. In the next step, we calculated m_i for each in-air measurement i using the $pO_2 - T$-slope a using

Eq. 3. As last step, we analyze the temporal trend of this m_i time series. For the short time period shown in this work, we chose a linear fit. For a longer analysis, a nonlinear fit or a combination of different linear fits should be considered. The drift due to biofouling, for example, cannot expected to be linear throughout an entire year.

Assessment

The SST and salinity of the five transects are shown in Fig. 1. During one transect, the measurements range from high temperatures up to 17°C and low salinities (down to 25) in the Skagerrak, decreasing temperatures with a salinity around 35 as one follows the transect westward, and low temperatures (2–5°C) with low salinities (around 31–32) as soon as one reaches the East Greenland Current. Very low salinities were observed on the fjord of Nuuk (down to 25). Between September 9th and September 12th, the vessel sailed into the long Kangerlussuaq fjord, where the measured salinities reached 0.

The pH_2O calculated from (1) optode temperature, (2) SST, and (3) air temperature and humidity from the NCEP/DOE AMIP-II reanalysis is shown in Fig. 3. Figure 3 also shows the effect of these three different methods on the $pO_{2;\ air}$ and the observed optode drift $1/m_i$. Overall method 1 gives larger values for pH_2O and the warming of the optode due to the higher temperature inside the vessel is also clearly visible. This results in an up to 7 hPa larger pH_2O (up to 4 hPa lower pO_2) for method 1 than method 2. For the open ocean, method 2 and 3 give relatively similar results. In coastal regions, especially toward the European shelf the pH_2O calculated after method 2 and 3 diverges largely. This is caused by unrealistically low temperatures in the NCEP/DOE AMIP-II reanalysis which is likely an artifact of the large grid size. The lower temperature results in an up to 25% lower pH_2O estimated by (3) (about 0.5–1% change in pO_2). Based on our data set, we determined the a $pO_2 - T$-slope a to be $a_{opt} = (0.0906 \pm 0.0085)$ hPa° C^{-1} for method 1 (method 2: $a_{SST} = (0.161 \pm 0.013)$ hPa° C^{-1} and method 3:$a_{NCEP/DOE\ II} = (0.221 \pm 0.016)$ hPa° C^{-1}). These are relatively low values, and fit well within the values reported for multipoint calibrated optodes (Bittig et al. 2018*b*). However, considering that this optode experiences a temperature range between 0°C and 20°C during deployment even the smallest value for a (method 1) has a large influence on the final pO_2 (1.8 hPa for 20°C temperature difference). Using the $pO_2 - T$-slope a, we calculated $1/m_i$ for every in-air measurement i and fitted this time series to estimate the average drift $1/m$. When looking at the $1/m_i$ time series determined for the three methods, we can see that using method 1 significantly reduces the noise and uncertainty of the fit compared to the two other methods. We found the time series slope of the sensor to be $1/m_{opt} = (-3.85 \pm 0.26)$ % yr^{-1}, $1/m_{SST} = (-3.81 \pm 0.53)$ %

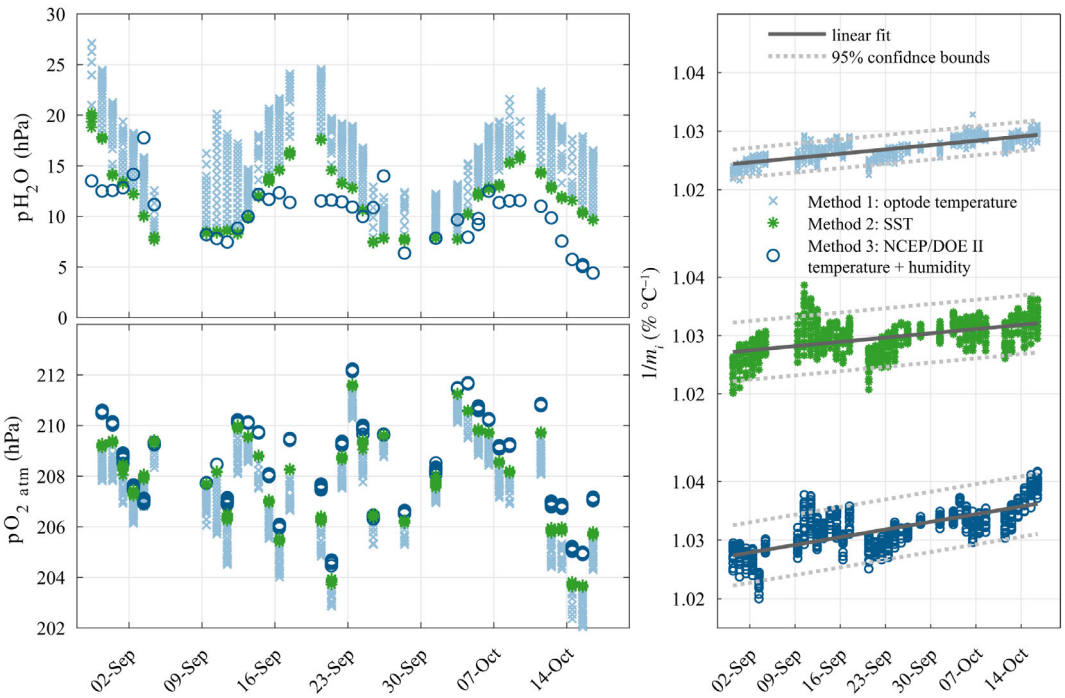

Fig. 3. Time series pH_2O, $pO_{2;\ air}$ and $1/m_i$ with linear regression (dark gray lines) calculated for the three different methods (method 1: Optode temperature [light blue], method 2: SST [green], method 3: Temperature and humidity from NCEP/DOE II reanalysis [dark blue]). The 95% confidence bounds (dashed lines) of the linear regression correspond to an error of two times the standard deviation.

yr^{-1}, and $1/m_{NCEP/DOE\ II} = (-6.83 \pm 0.55)\ \%\ yr^{-1}$. The uncertainty refers to a 95% confidence interval (two times the standard deviation).

For method 1, each of the five transects seems to have slightly larger drift within itself than the overall drift and it seems as if every second transect starts slightly lower than the transect before ended. This is likely a result of changing biofouling when the optode was running dry for 2–3 d during port stays in Aalborg, Denmark (around September 18th and October 10th). When looking at the single transects of the $1/m_i$ time series from method 2 and 3, we see a different drift behavior. While the overall drift does not differ much from the one determined for method 1, each transect shows a small temperature-dependent drift with lower $1/m_i$ at high temperatures and higher $1/m_i$ at low temperatures. This leads together with the larger spread during each measurement cycle (reflected in the larger noise) to the conclusion, that there is a remaining temperature effect in method 2 and 3, that we did not properly compensated for, although a_{SST} and $a_{NCEO/DOE\ II}$ are already larger than a_{opt}. This is likely an effect of changes in the pH_2O foil due to the warming of the optode and the optode housing. We therefore decided to use method 1 for all further calculation. There is potential for improving the representation of the drift through applying a set of linear regressions, one for each 3 week period (August 28th to September 18th, September 20th to October 8th, after October 10th). However, as the difference in calculated drift was very small, and such a procedure also introduces a risk for overfitting, we decided to rather use only one, but better constrained regression.

The drift rate determined from pre- and postcalibration conducted by Aanderaa, was determined as $d = (-2.84 \pm 0.15)\ \%\ yr^{-1}$ O_2 saturation. This is the average drift for the period May 2018–March 2019 based on calibration runs between 0°C and 20°C. A comparison of data corrected by the postcalibration, corrected by the in-air calibration, and without any drift correction can be found in Fig. 4. The drift determined from pre- and postcalibration is lower than the one determined from the in-air measurements which can have two reasons. First, we did not perform any temperature correction on this, and second, the drift of the optode is a combined effect of sensor intern drift and drift due to biofouling. We do not expect the biofouling component of the drift to be linear throughout the year. During the productive season, we expect a larger drift than during winter, which is in good agreement with our results.

Discussion

In Bittig et al. (2018*a*), the time series slope $1/m_t$ was found to be between −0.6 and + 0.6 % yr^{-1} for batch calibrated optodes and −0.4 to +0.2% yr^{-1} for individual multipoint calibrated optodes. These values are much lower than both, the drift we found in the in-air measurements ([−3.85 ± 0.26] % yr^{-1}) as well as the drift calculated from the postcalibration of our optode ([−2.84 ± 0.15] % yr^{-1}). On Nuka Arctica, we have had an optode installed since 2015 and we commonly observed drifts of about 3% yr^{-1}. The increased drift compared to float applications can be explained by the different deployment characteristics. During a deployment on a SOOP, the optode is performing much more measurements per year than most float-mounted do. Thus, a sensitivity loss due to the number of measurements will result in a larger drift in our application. However, the influence of the predeployment drift as well as the influence of biofouling plays most likely a larger role. Floats usually spend a lot of time at depth while waiting for their next profile. Our optode was exposed to surface seawater during the entire deployment which makes it more prone to biofouling.

In our application, we have to separate between two sources of biofouling. The first one is respiration in the pipe. This is a known problem in some underway systems (Juranek et al. 2010) and can lead to reduced O_2 readings during water measurements. This is not seen by the in-air calibration and contributes therefore to the uncertainty of the final water O_2 measurements. In order to minimize this source of uncertainty, we have a very large water flow in the main pipes (around 50 L min^{-1} and a pipe length of about 3 m) and clean the small hoses leading to the optode regularly. Second, we observe a biofilm growing on the optode. We believe that respiration in this biofilm is the major reason why we observe a larger drift in the in-air measurements compared to the postcalibration. Another argument for biofouling on the foil playing a role during our deployment are the shorter term changes that can be observed in the in-air measurements (Fig. 3, upper right panel and in the in-air calibrated data in Fig. 4). We observed slightly larger drift for periods of 3 weeks, together with step changes during the port calls in Aalborg (18 September 2018–20 September 2018 and 08 October 2018–11 October 2018). During ports, call in Aalborg the water is usually turned off and the optode is running dry. Hence, this pattern can be explained as being the consequence of a respirative biofilm growing on the optode that is partly dying off during the dry periods in port. The biofilm might not behave in the same way in air as when submerged in water: (1) the fouling organism might be less productive during dry periods, resulting in higher O_2 readings; (2) the biofilm drying out might lead to cracks and gaps in the biofilm making it more permeable for oxygen, resulting in higher oxygen readings; and (3) the absence of water flowing along the optode foil might lead to an increased oxygen gradient in the biofilm and thus lower O_2 readings. (1) and (2) would result in underestimating the drift, while (3) would result in an overestimation of the drift when using in-air measurements for drift correction. For a final evaluation of this, one would need to reproduce and investigate such a biofilm in a laboratory environment. Based on our data, we can find evidence for all three: (1) the fact that the gain was increasing during most in-

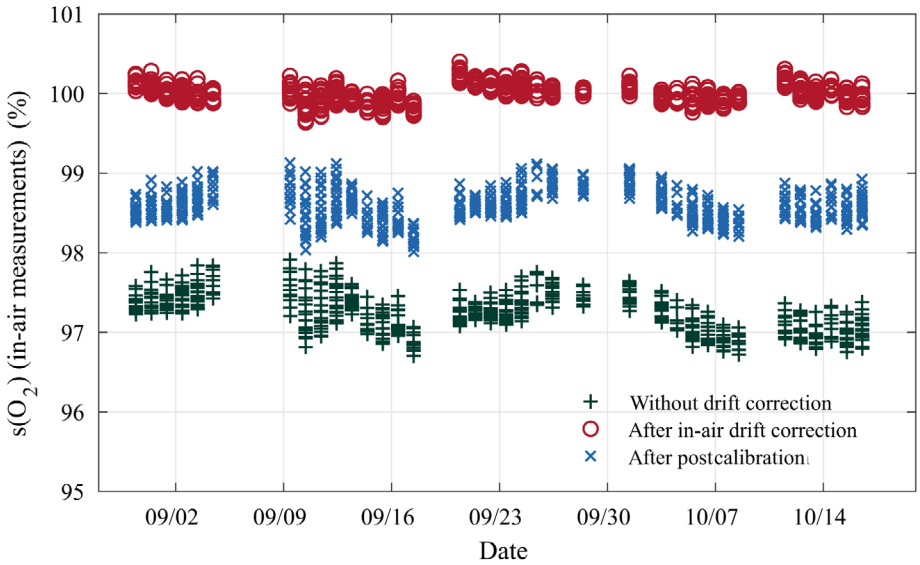

Fig. 4. Saturation oxygen of the in-air measurements without a drift correction (dark green), corrected with the in-air measurements (red), and with the post deployment calibration (blue).

air measurement periods support theory; (2) the step change during port calls in Aalborg where likely parts of the biofilm died aligns with theory; (3) while the fact that our calibrated measurements seem to slightly overestimate the oxygen saturation compared to Argo data (see below) can be an argument for theory.

As the drift of an optode in underway mode is a combination of sensor drift and drift due to biofouling, we cannot assume a linear drift throughout the year. Therefore, correcting the optode only using the postdeployment calibration might result in erroneous measurements. We expect the instrument to drift more when deployed in highly productive region as well as during spring and summer, which is in agreement with the larger drift determined from the in-air calibration than from the pre- and postcalibration during our deployment. An alternative method to account for different drift behavior during different seasons would be more frequent on-shore recalibration. How frequent this needs to be done depends on the region and season in which the sensor is deployed. For our instrument, recalibrating the optode in the lab every 1–2 months would be necessary. By using our in-air measurements, we can reduce the recalibration frequency to about once a year. Another method could be regular Winkler samples as a reference. In order to get reference samples over the entire range of temperatures and oxygen saturation, this requires the opportunity for joining the vessel and analyzing the samples in a laboratory soon after sampling. Both of these can be challenging in long-term underway installations.

The drift of optodes that are not constantly submerged in water was found to be up to several percent per year (D'Asaro and McNeil 2013). Using the in-air calibration system, we significantly improve the optode accuracy. We can determine the in-air drift of our optode with an uncertainty of $\pm$ 0.26%. This is in the same range as reached by the in-air calibrated optodes in float applications of $\pm$ 0.2% (Bushinsky et al. 2016). As there are some uncertainties remaining, related to possible influences of a biofilm growing on the optode and the estimation of the right pH_2O and respiration in the pipes, we estimate our accuracy to be around 3% for the final water measurements. For keeping the influence of respiration in the pipes small, we strongly recommend high water flow and a short piping system.

A comparison of the final oxygen concentration data with data obtained from Argo floats that surfaced nearby can be found in Fig. 5 (*see* Fig. 1 for the positions of the floats). We picked surface oxygen measurements from the profile that was closest in time to the vessel passing by. The maximal temporal difference between a profile and the underway data was set to 3 d. It is important to keep in mind that Nuka Arctica was sailing into the Kangerlussuaq fjord between September 9th and September 11th. The data measured during these days can therefore not be compared to the Argo data. The upper panel shows the oxygen saturation while the lower panel shows the oxygen concentration on both. Note that the oxygen saturation on the floats is calculated using standard pressure. The supersaturation measured on both platforms and its decrease toward October fits well with the climatology of the World Ocean Atlas 2018, which shows a slight supersaturation in September decreasing toward October as deep mixing in the region increases (Garcia et al. 2018). The average difference between our corrected oxygen concentration data and the float data was 5 $\pm$ 29 μmol kg^{-1} and –3.7% $\pm$ 2.4% for the saturation. These differences can have several reasons. First, we calculated the oxygen saturation of the Argo floats by using

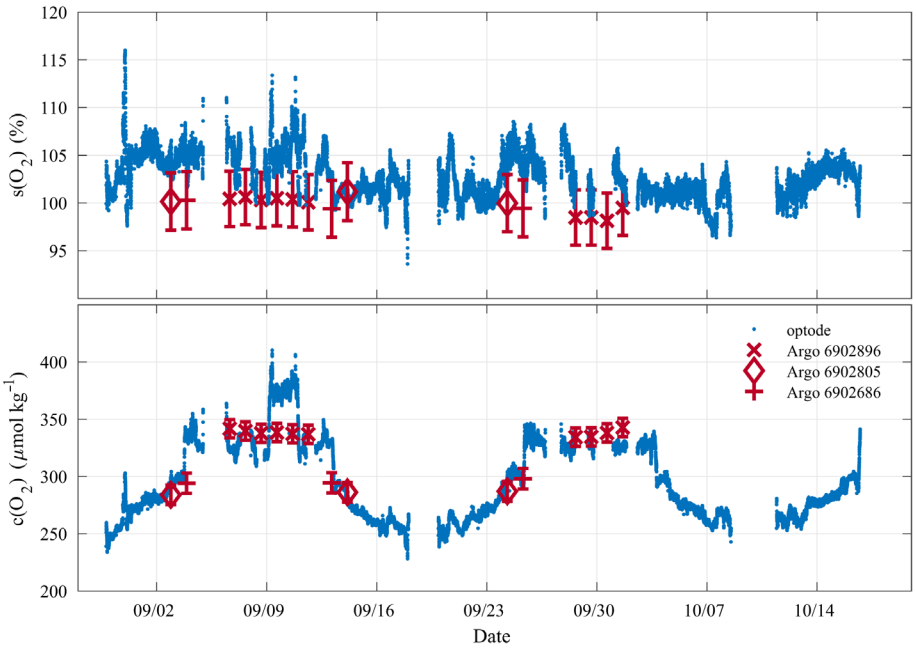

Fig. 5. Oxygen saturation (upper panel) and concentration (lower panel) of the underway measurements (blue) and three different Argo floats in the area (red). The error bars reflect the uncertainty of the Argo data (6902686, 6902805: 35; 6902896: 10 hPa).

standard pressure. Our pressure measurements on Nuka Arctica show longer periods with low atmospheric pressure, which can explain some of the high saturation measurements. We measured for example only around 1000 bar on September 4^{th}–11^{th}, which can explain a $\sim$ 1% higher oxygen saturation on the underway measurements. The steep increase of underway O_2 saturation from September 23^{rd} to September 25^{th} can, at least partly, be explained by a sudden decrease in air pressure from 1025 to 994 mbar. From October 13^{th}, we measured an air pressure of around 990 mbar causing the relatively large supersaturation measured during the last week of our measurements. Another reason for the differences between underway and Argo data can be biofouling within the underway system. However, respiration in the pipes would lead to a reduction in oxygen, which is not what we see in the comparison with the Argo data. Theory (3) as discussed above (an overcorrection of the in-air measurements due to an increased oxygen gradient in the biofilm as discussed above) could lead to systematically high oxygen readings. Finally, the spatial difference and the difference in SST associated to it can cause differences between the measurements of the two platforms. On Argo float 6902686, the float that matched best with the underway oxygen measurements, the temperature at sea surface was also closest to that measured on Nuka Arctica. In contrast to that, the SST on float 6902896 and 6902805 was 1–2° lower than those measured on Nuka Arctica. Increasing the temperature under constant oxygen concentration will lead to an about 2% higher oxygen saturation. This topic needs further investigation, for example, through deploying an underway in-air calibration system on a research vessel with the possibility to take reference samples, or by analyzing a much longer time series than the one we presented here.

Conclusions

Surface ocean oxygen concentration data can be used to, for example, estimate air–sea O_2 fluxes or net community production. For this, measurements with an accuracy of 0.5% are needed (Gruber et al. 2010). To achieve this, in situ air calibration routines were developed for float-mounted optodes, resulting in an accuracy of 0.2%.

We developed a system for in-air measurements of optodesin underway mode for use on SOOP vessels that operate a pCO_2 system or have similar installations. During the deployment, the sensor was exposed to a large range of temperature and salinity. By using these daily air measurements, we could reach an uncertainty of 3%. With a drift of -3.85 ± 0.26 % yr^{-1}, a proper drift correction is absolutely necessary for assuring high-quality oxygen data. The uncertainty could possibly be further decreased by fitting each transect separately, but for assessing this, a longer time series is needed. The here presented setup holds the potential to decrease the necessary frequency of sensor recalibration, while still delivering highly accurate measurements. This can hugely increase the impact of underway measurements of surface ocean oxygen concentration. We therefore recommend the use of in-air measurements after approach (1) in underway applications, if direct reference sampling is not possible. We

also recommend evaluating carefully for each deployment, whether a single linear regression or a set of linear regressions most accurately represents the drift behavior observed in the in-air measurements.

There are three major factors that can further increase the accuracy of the in-air calibrations: minimizing the warming that the optode undergoes once the seawater is turned off, better controlling the humidity in the air around the optode during the in-air analyses and further investigating the influence of biofouling. The warming is largely a consequence of the instrument being installed the engine room, which can run hot. Installing these instruments in colder rooms is often not feasible as the system also needs access to seawater and a seawater drain. One solution could be to design a water jacketed housing for the optode, which can reduce the warming during the in-air measurements. This will also improve the characterization of the humidity in the optode housing as it reduces evaporation. Another approach could be changing the installation in a way so that the air during the in-air measurements is not drained into the drain tank but teed off and measured by a humidity sensor instead. A third option could be to trap the air inside the optode housing during in-air measurements, so that it can reach 100% humidity. A long-term installation of the in-air calibration system on a research system with the possibility for regular reference sampling could be a good independent quality test. For achieving this, we have plans to install a similar system on the Norwegian research vessel G.O. Sars.

References

Alory, G., and others. 2015. The French contribution to the voluntary observing ships network of sea surface salinity. Deep-Sea Res. I Oceanogr. Res. Pap. **105**: 1–18. doi:10.1016/j.dsr.2015.08.005

Bakker, D. C. E., and others. 2016. A multi-decade record of high-quality fCO_2 data in version 3 of the Surface Ocean CO_2 Atlas (SOCAT). Earth Syst. Sci. Data **8**: 383–413. doi:10.5194/essd-8-383-2016

Bittig, H., and others. 2015. SCOR WG 142: Quality control procedures for oxygen and other biogeochemical sensors on floats and gliders. Recommendation for oxygen measurements from Argo floats, implementation of in-air-measurement routine to assure highest long-term accuracy. doi:10.13155/45917

Bittig, H., and others. 2018a. SCOR WG 142: Quality control procedures for oxygen and other biogeochemical sensors on floats and gliders. Recommendations on the conversion between oxygen quantities for Bio-Argo floats and other autonomous sensor platforms. Ifremer. doi:10.13155/45915

Bittig, H. C., and A. Körtzinger. 2017. Technical note: Update on response times, in-air measurements, and in situ drift for oxygen optodes on profiling platforms. Ocean Sci. **13**: 1–11. doi:10.5194/os-13-1-2017

Bittig, H. C., and others. 2018b. Oxygen optode sensors: Principle, characterization, calibration, and application in the ocean. Front. Mar. Sci. **4**: 429. doi: 10.3389/fmars.2017.00429

Bushinsky, S. M., and S. Emerson. 2013. A method for in-situ calibration of Aanderaa oxygen sensors on surface moorings. Mar. Chem. **155**: 22–28. doi:10.1016/j.marchem.2013.05.001

Bushinsky, S. M., S. R. Emerson, S. C. Riser, and D. D. Swift. 2016. Accurate oxygen measurements on modified Argo floats using in situ air calibrations. Limnol. Oceanogr.: Methods **14**: 491–505. doi:10.1002/lom3.10107

D'Asaro, E. A., and C. McNeil. 2013. Calibration and stability of oxygen sensors on autonomous floats. J. Atmos. Ocean. Technol. **30**: 1896–1906. doi:10.1175/JTECH-D-12-00222.1

Friederich, G. E., P. G. Brewer, R. Herlien, and F. P. Chavez. 1995. Measurement of sea surface partial pressure of CO_2 from a moored buoy. Deep-Sea Res. I Oceanogr. Res. Pap. **42**: 1175–1186. doi:10.1016/0967-0637(95)00044-7

Fröb, F., Olsen, A., Becker, M., Chafik, L., Johannessen, T., Reverdin, G., & Omar, A. (2019). Wintertime fCO2 variability in the subpolar North Atlantic since 2004. Geophysical Research Letters, **46**, 1580–1590. doi:10.1029/2018GL080554

Garcia, H. E., and others. 2018. World Ocean Atlas 2018, volume 3: Dissolved oxygen, apparent oxygen utilization, and oxygen saturation, p. 38. NOAA Atlas NESDIS.

Glueckauf, E. 1951. The composition of atmospheric air, p. 3–10.*In* H. R. Byers, H. E. Landsberg, H. Wexler, B. Haurwitz, A. F. Spilhaus, H. C. Willett, H. G. Houghton, and T. F. Malone [eds.], Compendium of meteorology: Prepared under the direction of the committee on the compendium of meteorology. American Meteorological Society.

Gruber, N. and others. 2010. Adding oxygen to Argo: Developing a global in situ observatory for ocean deoxygenation and biogeochemistry, p. 432–441. *In* Proceedings of OceanObs'09: Sustained Ocean Observations and Information for Society. European Space Agency. doi:10.5270/OceanObs09.cwp.39

Johnson, K. S., J. N. Plant, S. C. Riser, and D. Gilbert. 2015. Air oxygen calibration of oxygen optodes on a profiling float array. Journal of Atmospheric and Oceanic Technology, **32**: 2160–2172. doi:10.1175/JTECH-D-15-0101.1

Johnson, K. S., H. W. Jannasch, L. J. Coletti, V. A. Elrod, T. R. Martz, Y. Takeshita, R. J. Carlson, and J. G. Connery. 2016. Deep-Sea DuraFET: A pressure tolerant pH sensor designed for global sensor networks. Anal. Chem. **88**: 3249–3256. doi:10.1021/acs.analchem.5b04653

Johnson, K. S., and others. 2017. Biogeochemical sensor performance in the SOCCOM profiling float array. J. Geophys. Res. Oceans **122**: 6416–6436. doi:10.1002/2017JC012838

Juranek, L. W., R. C. Hamme, J. Kaiser, R. Wanninkhof, and P. D. Quay. 2010. Evidence of O_2 consumption in underway seawater lines: Implications for air-sea O_2 and CO_2 fluxes. Geophys. Res. Lett. **37**: L01601. doi:10.1029/2009GL040423

Körtzinger, A., J. Schimanski, and U. Send. 2005. High quality oxygen measurements from profiling floats: A promising new technique. J. Atmos. Ocean. Technol. **22**: 302–308. doi:10.1175/JTECH1701.1

Olsen, A., K. R. Brown, M. Chierici, T. Johannessen, and C. Neill. 2008. Sea-surface CO_2 fugacity in the subpolar North Atlantic. Biogeosciences **5**: 535–547. doi:10.5194/bg-5-535-2008

Pierrot, D., and others. 2009. Recommendations for autonomous underway pCO_2 measuring systems and data-reduction routines. Deep-Sea Res. II Top. Stud. Oceanogr. **56**: 512–522. doi:10.1016/j.dsr2.2008.12.005

Roemmich, D., and others. 2019. On the future of Argo: A global, full-depth, multi-disciplinary array. Front. Mar. Sci. **6**, 439. doi:10.3389/fmars.2019.00439

Takahashi, T. 1961. Carbon dioxide in the atmosphere and in Atlantic Ocean water. J. Geophys. Res. **66**: 477–494. doi:10.1029/JZ066i002p00477

Tengberg, D. A., J. Hovdenes, D. Barranger, O. Brocandel, R. Diaz, J. Sarkkula, C. Huber, and A. Stangelmayer. 2003. Optodes to measure oxygen in the aquatic environment. Sea Technol. **44**: 10–15.

Williams, N. L., and others. 2017. Calculating surface ocean pCO_2 from biogeochemical Argo floats equipped with pH: An uncertainty analysis. Global Biogeochem. Cycles **31**: 591–604. doi:10.1002/2016GB005541

Acknowledgment

The authors would like to thank crew, captains, and owner of M/V Nuka Arctica. Without their generous support, this study would not have been possible. This work was funded by the project ICOS Norway (Research Council of Norway, 245927). Salinity data were supplied by SNO SSS. We used NCEP Reanalysis 2 data provided by the NOAA/OAR/ESRL PSD, Boulder, Colorado, U.S.A., from their website at https://www.esrl.noaa.gov/psd/. The Argo data were collected and made freely available by the International Argo Project and the national programs that contribute to it (http://www.argo.net). Argo is a pilot program of the Global Ocean Observing System. We also want to thank the PIs and projects providing the Argo data used in this article: Virginie Thierry (6902686, RREX; 6902805, CORIOLIS) and Marcel Babin (6902896, NAOS - France).

Conflict of Interest

None declared.

Submitted 06 July 2020
Revised 27 November 2020
Accepted 28 January 2021

Associate editor: Mike DeGrandpre